HOKKAIDO UNIVERSITY

Title	Comparison of 99mTc-annexin A5 with 18F-FDG for the detection of atherosclerosis in ApoE-/- mice
Author(s)	Zhao, Yan; Kuge, Yuji; Zhao, Songji et al.
Citation	European Journal of Nuclear Medicine and Molecular Imaging, 34(11), 1747-1755 https://doi.org/10.1007/s00259-007-0433-2
Issue Date	2007-11
Doc URL	https://hdl.handle.net/2115/30199
Rights	The original publication is available at www.springerlink.com
Type	journal article
File Information	EJNMMI34-11.pdf

Hokkaido University Collection of Scholarly and Academic Papers : HUSCAP

Title: **Comparison of ^{99m}Tc-annexin A5 with ^{18}F-FDG for detecting atherosclerosis in ApoE-/- mice**

Authors:

Yan Zhao, MD[1], Yuji Kuge, PhD[2-4], Songji Zhao, MD[1, 2], Koichi Morita, MD[1], Masayuki Inubushi, MD[3], H. William Strauss, MD[5], Francis G. Blankenberg, MD[6], Nagara Tamaki, MD[1]

Affiliations:

[1]Department of Nuclear Medicine, Graduate School of Medicine, Hokkaido University, Sapporo, Japan

[2]Department of Tracer Kinetics, Graduate School of Medicine, Hokkaido University, Sapporo, Japan

[3]Department of Molecular Imaging, Graduate School of Medicine, Hokkaido University, Sapporo, Japan

[4]Department of Patho-functional Bioanalysis, Graduate School of Pharmaceutical Sciences, Kyoto University, Kyoto, Japan

[5]Department of Nuclear Medicine, Sloan-Kettering Cancer Center, New York, New York, United States

[6]Department of Pediatric Radiology, Stanford University School of Medicine, Palo Alto, California, United States

Communicating Author:

Nagara Tamaki, MD,PhD

Department of Nuclear Medicine

Graduate School of Medicine, Hokkaido University

North 15, West 7, Kita-ku, Sapporo 060-8638, JAPAN

Telephone: 81-11-706-5150; Fax: 81-11-706-7155

E-mail: natamaki@med.hokudai.ac.jp

ABSTRACT

Purpose: ^{99m}Tc-annexin A5, a marker of ongoing apoptosis and ^{18}F-FDG, a marker of the increased metabolism of inflammatory cells, are supposed to be useful in detecting metabolically active atheroma. This study reports a comparison of the intralesional distribution of these tracers in relation to lesion development in ApoE-/- mice. **Methods**: Male ApoE-/- mice (n=12-14/group) were maintained on a western-type diet after the age of 5-wks. At 25-wks, ^{99m}Tc-annexin A5 or ^{18}F-FDG was injected and the aortas were harvested for autoradiography (ARG) and Oil Red O staining. Regional radioactivity accumulation was compared in relation to the Oil Red O staining score (ranged from 0 to 3, a semiquantitative parameter for evaluating lesion development). **Results:** Both ^{99m}Tc-annexin A5 and ^{18}F-FDG showed preferential uptakes into atherosclerotic lesions, with higher uptake levels for ^{18}F-FDG (mean, 56.07 %ID x kg/m^2) than ^{99m}Tc-annexin A5 (mean, 10.38 %ID x kg/m^2). The regional uptake levels of these tracers were correlated with Oil Red O staining score ($r=0.65$, $P<0.05$ for ^{99m}Tc-annexin A5; $r=0.56$, $P<0.05$ for ^{18}F-FDG). The uptake ratios of

advanced lesions (score, > 0.5) to early lesions (score, < 0.5) were significantly higher for ^{99m}Tc-annexin A5 than ^{18}F-FDG (f=4.73, p=0.03). **Conclusions**: Both ^{99m}Tc-annexin A5 and ^{18}F-FDG accumulate in atherosclerotic lesions and significantly correlate with the severity of each lesion. The higher absolute uptake levels of ^{18}F-FDG may be advantageous for lesion detection, whereas the preferential uptake of ^{99m}Tc-annexin A5 in advanced lesions maybe a useful indicator of late stage lesions or vulnerable plaque transformation.

Key Words: atherosclerosis, apoptosis, ^{99m}Tc-annexin A5, ^{18}F-FDG, apolipoprotein E-knockout mouse.

INTRODUCTION

Atherosclerotic plaque rupture is a common cause of myocardial infarction and ischemic cerebrovascular accidents that remain as major causes of premature morbidity in developed countries [1-5]. The detection of vulnerable plaques is therefore clinically important for stratifying and providing early treatment. Several invasive and noninvasive imaging modalities are used to provide the necessary anatomic or functional information to identify plaques at risk of rupture [6-13]. Nuclear imaging has several advantages, including its noninvasive nature and its potential to quantify important determinants of plaque vulnerability based on specific cellular or biochemical changes that characterize these lesions.

Inflammation and apoptosis are important components of plaque vulnerability [14-17]. Because the metabolic and apoptotic signals are large, it is likely that even small lesions will be visible [18]. For these reasons, ^{99m}Tc-labeled annexin A5, a SPECT tracer as a marker of ongoing apoptotic cell death, and ^{18}F-FDG, a PET tracer as a marker of inflammation, are being evaluated for detecting vulnerable atherosclerotic plaques [18-23]. It

is unclear, however, which tracer is more useful for detecting atherosclerotic lesions and for determining lesion vulnerability.

Apolipoprotein E-knockout (ApoE-/-) mice have been widely used in studies of atherosclerosis, because they spontaneously develop hypercholesterolemia and atherosclerotic lesions similar to those found in humans [24,25]. Recently, some investigators have also observed spontaneous plaque rupture in the brachiocephalic arteries and subsequent sudden death in aged ApoE-/- mice [26-29]. These data suggest that ApoE-/- mice could be a useful model for the evaluation of tracers for detecting unstable atherosclerotic lesions.

This study reports our findings of the intralesional distribution of ^{99m}Tc-annexin A5 and ^{18}F-FDG in ApoE-/- mice.

MATERIALS AND METHODS

Preparations of ^{99m}Tc-annexin A5 and ^{18}F-FDG

Recombinant (rh) human annexin A5 was produced by expression in *Escherichia coli* as previously described [13, 30-31]. Rh-annexin A5 was derivatized with hydrazinonicotinamide (HYNIC) and then labeled with ^{99m}Tc with tricine as coligand as described previously (specific activity: 4.8 MBq/μg protein) [32]. ^{18}F-FDG was obtained from Hokkaido University hospital which produces the tracer for clinical use.

Animal Studies

Animal care and all experimental procedures were performed under the approval of the Animal Care Committee of Hokkaido University.

Studies were performed on ApoE-/- mice (n=12-14/group) and wild-type mice (C57BL/6J: n=11-15/group), respectively obtained from Taconic's Gnotobiotic Center (Germantown, NY) and CLEA JAPAN Inc. (Tokyo, Japan). All animals were kept in a temperature-controlled facility in the Laboratory of Animal Experiments at Hokkaido University, on a 12-hour

light and 12-hour dark cycle with free access to food and water. From the age of 5-wks, the animals were maintained on a high-fat western type diet (21% fat, 0.15% cholesterol, no cholate; diet # TD88137, Harland Teklad). At the age of 25-wks the animals were fasted, anesthetized with pentobarbital anesthesia (0.025 mg/kg, intraperitoneally) and either ^{99m}Tc-annexin A5 (18.5 MBq/mouse) or ^{18}F-FDG (18.5 MBq/mouse) was injected to both ApoE-/- and control mice. Blood glucose levels of all animals were measured immediately before the injection. Two hours after ^{99m}Tc-annexin A5 injection or 1 hour after ^{18}F-FDG injection, blood samples (0.9 to 1.5 ml per mouse) were collected under deep anesthesia for subsequent analysis of cholesterol and triglyceride levels. The aorta was fixed by cardiac perfusion with cold 0.1 M phosphate buffer solution (pH 7.4) followed by cold fixative (4% paraformaldehyde, 0.1 M phosphate buffer solution (pH 7.4), removed and mounted on a clean glass slide after longitudinal incision.

Autoradiographic Studies

To visualize the distribution of each tracer in the aorta, the specimens were exposed to phosphor imaging plates (Fuji Imaging Plate BAS-UR, Fuji Photo Film, Japan) for 2 hours in ^{18}F-FDG examination and for 12 hours in ^{99m}Tc-annexin A5 examination, together with a set of calibrated standards [33, 34]. The autoradiographic images were analyzed using a computerized imaging analysis system (Fuji bio-imaging analyzer BAS5000). To quantify the regional uptake levels of ^{99m}Tc-annexin A5 and ^{18}F-FDG, regions of interest (ROIs; 0.36 mm^2) were placed over the entire surface area of the ARG images (Figure 1A). The radioactivity in each ROI was shown by photostimulated luminescence per unit area (PSL=a*D*t: a, constant; D, radioactivity exposed on imaging plate; t, exposure time). Each count of PSL/mm^2 from the aortic tissues was recorded and converted to percentage injected dose per m^2 of aortic tissue surface area (%ID/m^2) using the activity of the standards. The data were normalized by animal body weight (%ID x kg/m^2). To determine the relative tracer uptake level in advanced lesions to early lesions, relative uptake values (RUVs) were defined as the ratio of

tracer uptake in each ROI group to that in the ROI group with Oil Red O staining scores of 0-0.5 (see below).

Histological Studies

The same aortic tissues that were used for autoradiographic analysis were carefully stained with Oil Red O (Sigma) to coordinate with the autoradiograms. Briefly, the aortic tissues were rinsed with 60% 2-propanol for 3 min, incubated in Oil Red O solution at 37°C for 40 min, then destained in 60% 2-propanol for 6 min and mounted on glass slides using aqueous mounting medium (Biomeda corporation, Foster city, California). For histological grading, the ROIs defined on the autoradiograms were transferred to the histological images. The Oil Red O stained specimens were microscopically examined and the intensity of staining and percentage of positively stained area were determined in each ROI. The intensity of staining was graded from 0 to 3 (0 = not stained, 1 = slightly stained, 2 = intensely stained, 3 = very intensely stained) (Figure 1 B-E). The atherosclerosis severity levels were assessed semiquantitatively using the

product of these scores (intensity x % positive area; Oil Red O staining score). On the basis of the Oil Red O staining score, ROIs were divided into three ROI groups (Oil Red O staining scores: 0 to 0.5, 0.5 to 1, and more than 1). For testing feasibility of the histological grading based on Oil Red O staining, hematoxylin and eosin staining and immunohistochemical staining with the mouse macrophage specific antibody (Mac-2, clone m3/38, Cedarlane, Ontario, Canada) were performed with standard procedures [34] using several aortic specimens embedded in paraffin (Figure 1).

Statistical Analysis

All numerical parameters were expressed as mean ± SD. Unpaired Student's *t* test was performed to evaluate the significance of differences in body weight, blood glucose level, and plasma lipid level between ApoE-/- and control mice and between ^{99m}Tc-annexin A5 and ^{18}F-FDG groups (Table 1). The differences in the average uptake levels of ^{99m}Tc-annexin A5 and ^{18}F-FDG in the aortic tissues between the ApoE-/- and control mice were also tested using unpaired Student's *t*-test (Figure 3). Repeated measures

ANOVA was performed to evaluate the significance of differences in atherosclerotic lesion development (Table 2) and relative uptake values (RUVs) (Figure 5) between ^{99m}Tc-annexin A5 and ^{18}F-FDG groups. The correlation between the Oil Red O staining score and the regional tracer levels was assessed by spearman's correlation coefficient by rank. One-way ANOVA followed by post-hoc analysis (Bonferroni) was performed to evaluate the significance of differences in the regional tracer levels among the ROI groups with different Oil Red O staining scores (Figure 4). A two-tailed $P < 0.05$ was considered statistically significant.

RESULTS

Body Weight, and Blood Glucose and Plasma Cholesterol Levels

The body weight, and blood glucose and plasma lipid levels of ApoE-/- and control mice are shown in Table 1. Significantly higher body weight and plasma lipid levels were observed in ApoE-/- mice compared with the corresponding control mice. The blood glucose levels were significantly higher in control mice than in ApoE-/- mice. No significant difference was observed in each parameter between ^{99m}Tc-annexin A5 and ^{18}F-FDG groups in the same strain.

Histological Studies

Table 2 shows the summary of the atherosclerotic lesions developed in the ApoE-/- and control mice. In the ApoE-/- mice, various atherosclerotic changes, from early to advanced lesions, were observed throughout the aortic tissues. The advanced lesions were predominantly located at the branch of the thoracic aorta to the right carotid artery and lesser curvature of the aortic arch. No significant differences were observed in the

atherosclerotic lesion development between the ^{99m}Tc-annexin A5 group and the ^{18}F-FDG group (f=0.76; p=0.48). No obvious atherosclerotic changes were observed in the aorta of control mice.

Autoradiographic Studies

Figure 2 shows the autoradiograms and corresponding Oil Red O stained aortas of ApoE-/- mice injected with ^{99m}Tc-annexin A5 or ^{18}F-FDG. These tracers preferentially accumulated into the regions stained with Oil Red O.

Figure 3 shows the average uptake levels (%ID x kg/m^2) of ^{99m}Tc-annexin A5 and ^{18}F-FDG in the aortic tissues of ApoE-/- and control mice. Both ^{99m}Tc-annexin A5 and ^{18}F-FDG uptake levels were significantly higher in ApoE-/- mice, which were nearly 2-fold greater than that of the corresponding control animals (10.38±3.16 vs. 5.28±1.19 for ^{99m}Tc-annexin A5 groups, and 56.07±29.94 vs. 29.42±19.07 for ^{18}F-FDG groups). The ^{18}F-FDG uptake levels in the aortic tissues were markedly higher than those of ^{99m}Tc-annexin A5 in both strains.

Relationship between Regional Tracer Uptake and Lesion Development

Figure 4 shows the correlation between regional tracer uptake levels and lesion development in ApoE-/- mice. For both tracers, the regional tracer uptake levels in the aortic tissues were correlated with the severity of atherosclerotic changes determined by the Oil Red O staining. ^{99m}Tc-annexin A5 accumulation showed better correlation with the severity of atherosclerotic changes ($r=0.65$; $p<0.05$) than that of ^{18}F-FDG ($r=0.56$, $p<0.05$). The uptake level of ^{99m}Tc-annexin A5 in the region with atherosclerotic severity scores from 0 to 0.5 was significantly lower than those in any other regions with higher Oil Red O staining scores (0.5 to 1.0 and more than 1.0), whereas the differences in ^{18}F-FDG uptake level were not significant.

The tracer uptake ratios of advanced to early lesions are shown in Figure 5. ^{18}F-FDG showed relatively low uptake ratios for advanced lesions with higher Oil Red O staining scores (more than 0.5), because of a relatively high uptake in early lesions scored 0 to 0.5. The uptake ratios of

^{99m}Tc-annexin A5 for advanced lesions scored 0.5 to 3 were significantly higher than those of ^{18}F-FDG (f=4.73; p=0.03).

DISCUSSION

This study was designed to verify the usefulness of ^{99m}Tc-annexin A5 and ^{18}F-FDG to image and quantify atherosclerotic lesion progression in a spontaneous atherosclerosis animal model (ApoE-/- mice). Widespread atherosclerotic lesions developed in the hypercholesterolemic mice after 20 weeks of high-fat feeding. The variation of Oil Red O staining allowed us to stratify the lesions to those with high and low lipid content which partly indicated the levels of atherosclerosis progression. Both ^{99m}Tc-Annexin A5 and ^{18}F-FDG showed preferential uptakes into atherosclerotic lesions, with higher uptake levels for ^{18}F-FDG than for ^{99m}Tc-Annexin A5. The regional levels of both tracers were correlated with the severity of atherosclerotic changes as demonstrated by Oil Red O staining, and the uptake ratios of advanced to early lesions were significantly higher for ^{99m}Tc-annexin A5 than for ^{18}F-FDG. These results indicate that the aortic accumulations of

^{99m}Tc-annexin A5 and ^{18}F-FDG increased with the progression of atherosclerosis. The higher absolute uptake levels of ^{18}F-FDG may enhance lesion detection, whereas the preferential uptake of ^{99m}Tc-annexin A5 in advanced lesions maybe a useful indicator of late stage lesions or transformation to vulnerable plaques.

In human arterial tissues, atherosclerotic lesions develop and progress slowly throughout life. Vulnerable plaque rupture induces outbreaks of sudden cardiac death, myocardial infarction and other acute obstructive vascular diseases. To prevent the occurrence of these diseases, it is essential to clarify the atherosclerotic lesion progression from benign lesions to their conversion into vulnerable plaques. In this regard, several previous studies demonstrated the detection of plaque instability using ^{99m}Tc-annexin A5 or ^{18}F-FDG in human and animal models of atherosclerosis [19-23, 35-38]. However, it remains to be elucidated which tracer is more useful for detecting atherosclerotic lesions and for determining lesion vulnerability. From our comparison between the two tracers, ^{99m}Tc-annexin A5 showed higher correlation between regional tracer uptake level and atherosclerotic

severity (r=0.65; p<0.05) than that of ^{18}F-FDG (r=0.56, p<0.05). More importantly, the significantly higher uptake levels of ^{99m}Tc-annexin A5 in advanced lesions (Figure 4) indicate the potential of this tracer to identify plaques with higher risk of rupture. The uptake ratios of advanced to early lesions were significantly higher for ^{99m}Tc-annexin A5 than for ^{18}F-FDG (Figure 5). On the other hand, ^{18}F-FDG showed significantly higher absolute uptake levels in the aortic tissues than those of ^{99m}Tc-annexin A5, suggesting that ^{18}F-FDG may be more sensitive for detecting plaques of different severities. The high image resolution and sensitivity of PET also enhance the detectability of small objects such as atherosclerotic plaques. It may be possible to take advantage of the superior characteristics of PET imaging with Annexin-A5, by labeling the protein with either fluorine-18 [39] or gallium-68 [40]. Closing up a radiation detector to the atherosclerotic lesions by using intravascular catheter can also be a considerable alternative method to detect the small lesions [37]. Thus, our study using ApoE-/- mice clearly characterized the potential of these tracers.

For ^{99m}Tc-annexin A5, Kolodgie et al. [23] have imaged experimental

atheroma using a rabbit model with balloon-injured abdominal aorta. They demonstrated a significant correlation (r=0.47, p=0.04) between tracer accumulation and histologically verified macrophage apoptosis, and the mean %ID/g uptake was significantly higher in aortic segments with AHA type IV lesion than in aortic segments with AHA type II or type III lesions. Johnson et al. [35] have imaged experimental atherosclerotic lesions using a juvenile swine model with balloon-injured coronary vessels. Isobe S et al. [38] have imaged spontaneous atherosclerotic lesions in high-fat feeding ApoE-/- mice and LDL-/- mice with micro-SPECT/CT. They demonstrated a significant correlation between ^{99m}Tc-annexin A5 uptake and both macrophage infiltration and the extent of apoptosis. The results of our study are in agreement with those of previous studies. For ^{18}F-FDG, Ogawa et al. [22] using atherosclerotic rabbits has confirmed a close correlation between ^{18}F-FDG uptake level and macrophage number in atherosclerotic plaques (r=0.81), suggesting that ^{18}F-FDG has the potential for identifying macrophage-rich unstable lesions. Other investigations in balloon-injured aortas [19, 41] or symptomatic plaques obtained by carotid endarterectomy

(CEA) [42] also confirmed that ^{18}F-FDG uptake reflecting macrophage infiltration in atherosclerotic lesions. In our study, however, the correlation between ^{18}F-FDG uptake level and atherosclerotic lesion development was relatively weak, compared with the results from the above-mentioned studies. The differences in the lesion characteristics of animal models and approaches to analysis the lesion severity may explain the discrepancy. In this study, we used Oil Red O for staining lipid deposits inside atherosclerotic lesions for histological examination, instead of counting the number of cellular components.

It is also important to consider the methodological aspects used in this study. We used ApoE-/- mice, a type of spontaneous atherosclerosis animal model, which develop atherosclerotic lesions slowly in its aortic tissues throughout the whole arterial tree. Several publications have been issued recently which demonstrated the vulnerability of plaques in apoE-/- mice, especially in the high-fat feeding apoE-/- mice [26-29]. Intramural bleeding was also reportedly observed in the brachiocephalic arteries at an older age (60 weeks old) possibly caused by plaque rupture [43]. Various

atherosclerotic changes, from early to advanced lesions, were observed in the aortic tissues in our mice, which allowed us determine tracer uptake levels in relation to lipid deposition in the atheroma. On the other hand, apoE -/- mice have impairment in lipid metabolism, which may affect glucose metabolism and may result in altered tracer distribution, particularly ^{18}F-FDG distribution. Several experimental evidences, however, showed that apoE -/- mice were resistant to developing hyperglycemia in response to high-fat, even diabetogenic diet [44]. In fact, the plasma glucose levels in our apoE -/- mice were within a normal range. Accordingly, it is unlikely that impairment of lipid metabolism in apoE -/- mice significantly affect the tracer accumulation in this study.

One major disadvantage of this study is the separate investigations of ^{99m}Tc-annexin A5 and ^{18}F-FDG, which hampered the simultaneous comparison of the difference in the uptake levels of these two tracers in the same atherosclerotic lesion and animal. A dual-tracer study using ^{99m}Tc-annexin A5 and ^{18}F-FDG in the same animal will provide more precise comparison between these two tracers. It should also be noted that

the autoradiographic images were taken by mounting the whole aorta on a slide after longitudinal incision. The thickness of the aorta may affect the quantitative determination of the tracer distribution, as the thickness can be changed due to the atherosclerotic progression state. In spite of this limitation, this method is widely used and well established to examine the fesibility of radiolabeled agents for detecting atheorsclerotic lesions [45, 46], and the imaging intensity also matched with the quantitative tissue counting result [47]. Thus, this method helps us compare the tracer distribution in the whole aorta with the histological evaluation, although careful interpretation of the autoradiogaraphic images is strongly required. Another disadvantage may be an insufficient histological evaluation. In the present study, we used Oil Red O staining with the purpose of documenting the atherosclerosis progression throughout the entire aorta and correlated it with the tracer accumulation. The Oil Red O staining is commonly used for identifying exogenous or endogenous lipid deposits. From the early stages of lesion formation while lipid-filled macrophages appear in the subendothelium, to the advanced stages while macrophage degeneration and the formation of

lipid pools or necrotic core, the lesion development in ApoE-/- mice was accompanied with the increase of lipid contents [29]. More importantly, during the destabilization of plaques, the increase of lipid content is accompanied with the increase of macrophage [48, 49], and the lipid content in vulnerable plaques is significantly higher than that of stable lesions [27]. Accordingly, the intensity of Oil Red O stain is a reasonable parameter that can be used for evaluating the lesion development, which was also confirmed by hematoxylin and eosin staining and immunohistochemical staining for macrophage (Figure 1). However, more detailed histological information on lesion development such as lesion structure or inflammatory cell density is required to clarify the changes in tracer uptake levels with the changes of cellular components inside atherosclerotic lesions. In the present study, autoradiographic images of the whole aorta were taken after longitudinal incision, to compare the tracer distribution in the whole aorta with the histological evaluation, which hampered the performance of detailed cross sectional staining.

CONCLUSION

Our findings in a mouse model of spontaneous atherosclerosis verified the usefulness of ^{99m}Tc-annexin A5 and ^{18}F-FDG as nuclear imaging agents for detecting atherosclerotic lesions. High absolute uptake level in aortic tissues and fluorine-18 labeling of ^{18}F-FDG may offer higher sensitivity in lesion detection, whereas the preferential uptake of ^{99m}Tc-annexin A5 in advanced lesions suggests its potential for assessing the vulnerability of atherosclerotic plaques.

ACKNOWLEDGMENTS

This research was supported in part by Grant-in-Aid for General Scientific Research from the Ministry of Education, Culture, Sports, Science and Technology of Japan and from the Japan Society for the Promotion of Science and by a research grant for cardiovascular diseases from the Ministry of Health, Labour and Welfare (15C-5 and 16C-8). The authors would like to thank the staff members of the Department of Nuclear Medicine and Central Institute of Isotope Science, Hokkaido University, and Facility of Radiology, Hokkaido University Medical Hospital for supporting this work. We also thank Theseus Imaging Corporation for providing annexin A5.

REFERENCES

1. Virmani R, Burke AP, Kolodgie FD, Farb A. Pathology of the thin-cap fibroatheroma: a type of vulnerable plaque. J Interv Cardiol. 2003 Jun; 16: 267-72.

2. Virmani R, Kolodgie FD, Burke AP, Farb A, Schwartz SM. Lessons from sudden coronary death: a comprehensive morphological classification scheme for atherosclerotic lesions. Arterioscler Thromb Vasc Biol. 2000; 20:1262-75.

3. Ross R. The pathogenesis of atherosclerosis: a perspective for the 1990s. Nature. 1993; 362:801-809.

4. Hamm CW, Bertrand M and Braunwald E. Acute coronary syndrome without ST elevation: implementation of new guidelines. Lancet. 2001; 358:1533-1538.

5. John RD, James FR, Tim DF and Peter LW. Targeting the vulnerable plaque: The evolving role of nuclear imaging. J Nucl Med. 2005; 12:234-246.

6. Nissen SE and Yock P, Intravascular ultrasound novel

pathophysiological insights and current clinical applications. Circulation. 2001; 103:604–616.

7. Yabushita H, Bouma BE, Houser SL, Aretz HT, Jang IK and Schlendorf KH et al. Characterization of human atherosclerosis by optical coherence tomography. Circulation. 2002; 106:1640–1645.

8. Stefanadis C, Diamantopoulos L, Vlachopoulos C, Tsiamis E, Dernellis J and Toutouzas K et al. Thermal heterogeneity within human atherosclerotic coronary arteries detected in vivo: A new method of detection by application of a special thermography catheter. Circulation. 1999; 99:1965–1971.

9. Waki H, Masuyama H, Mori H, Maeda T, Kitade K and Moriyasu K et al. Ultrasonic tissue characterization of the atherosclerotic carotid artery: Histological correlates or carotid integrated backscatter. Circ J. 2003; 67:1013–1016.

10. Schroeder S, Kopp AF, Baumbach A, Meisner C, Kuettner A and Georg C et al. Noninvasive detection and evaluation of atherosclerotic coronary plaques with multislice computed tomography. J Am Coll

Cardiol. 2001; 37:1430–1435.

11. Yuan C, Kerwin WS, Ferguson MS, Polissar N, Zhang S and Cai J et al. Contrast-enhanced high resolution MRI for atherosclerotic carotid artery tissue characterization. J Magn Reson Imaging. 2002; 15:62–67.

12. Trivedi RA, King-Im JM, Graves MJ, Cross JJ, Horsley J and Goddard MJ et al. In vivo detection of macrophages in human carotid atheroma: Temporal dependence of ultrasmall superparamagnetic particles of iron oxide-enhanced MRI. Stroke. 2004; 35:1631–1635.

13. Blankenberg FG, Katsikis PD, Tait JF et al. In vivo detection and imaging of phosphatidylserine expression during programmed cell death. Proc Natl Acad Sci USA. 1998; 95:6349–6354.

14. Ross R. Atherosclerosis: an inflammatory disease. N Engl J Med. 1999; 340:115-126.

15. Van der Wal AC, Becker AE, Van der Loss CM and Das PK. Site of intimal rupture or erosion of thrombosed coronary atherosclerotic plaques is characterized by an inflammatory process irrespective of dominant plaque morphology. Circulation. 1994; 89:36-44.

16. Geng YJ and Libby P. Evidence for apoptosis in advanced human atheroma. Am J Pathol. 1995; 147:251-266.

17. Lendon CI, Davies MJ, Born GV et al. Atherosclerotic plaque caps are locally weakened when macrophage density is increased. Atherosclerosis. 1991; 87:87-90.

18. Strauss HW, Grewal RK, Pandit-Taskar N. Molecular imaging in nuclear cardiology. Semin Nucl Med. 2004 Jan; 34(1):47-55.

19. Tawakol A, Migrino RQ, Hoffmann U, Abbara S, Houser S, Gewirtz H, Muller JE, Brady TJ, Fischman AJ. Noninvasive in vivo measurement of vascular inflammation with F-18 fluorodeoxyglucose positron emission tomography. J Nucl Cardiol. 2005 May-Jun; 12(3):294-301.

20. Lederman RJ, Raylman RR, Fisher SJ, Kison PV, San H and Nabel EG. Detection of atherosclerosis using a novel positron-sensitive probe and 18-fluorodeoxyglucose (FDG). Nucl Med Commun. 2001; 22:747-753.

21. Rudd JHF, Warburton EA, Fryer TD, Jones HA, Clark JC and Antoun N. Imaging atherosclerotic plaque inflammation with [^{18}F]-fluorodeoxyglucose positron emission tomography. Circulation.

2002; 105:2708-2711.

22. Ogawa M, Ishino S, Mukai T, Asano D, Teramoto N and Watabe H. (18)F-FDG accumulation in atherosclerotic plaques: Immunohistochemical and PET imaging study. J Nucl Med. 2004; 45:1245-1250.

23. Kolodgie FD, Petrov A, Virmani R, Narula N, Verjans JW and Weber DK. Targeting of apoptotic macrophages and experimental atheroma with radiolabeled annexin V: A technique with potential for noninvasive imaging of vulnerable plaque. Circulation. 2003; 108:3134-3139.

24. Plump AS, Smith JD, Hayek T et al. Severe hypercholesterolemia and atherosclerosis in apolipoprotein E-dificient mice created by homologous recombination in ES cells. Cell. 1992; 71:343-353.

25. Zhang SH, Reddick RL, Piedrahita JA and Maeda N. Spontaneous hypercholesterolemia and arterial lesions in mice lacking apolipoprotein E. Science. 1992; 258:468-471.

26. Johnson JL, Jackson CL. Atherosclerotic plaque rupture in the apolipprotein E knockout mouse. Atherosclerosis. 2001; 154 (2):

399-406.

27. Williams H, Johnson JL, Carson KGS and Jackson CL. Characteristics of intact and ruptured atherosclerotic plaques in the brachiocephalic arteries of apolipoprotein E knockout mice. Arterioscler Thromb Vasc Biol. 2002; 22: 788–792.

28. Johnson J, Carson K, Williams H et al. Plaque rupture after short periods of fat feeding in the apolipoprotein E-knockout mouse: model characterization and effects of pravastatin treatment. Circulation. 2005 Mar 22; 111(11):1422-30.

29. Coleman R, Hayek T, Keidar S and Aviram M. A mouse model for human atherosclerosis: long-term histopathological study of lesion development in the aortic arch of apolipoprotein E-deficient (E0) mice. Acta Histochem. 2006;108(6):415-24.

30. Wood BL, Gibson DF and Tait JF. Increased erythrocyte phosphatidylserine exposure in sickle cell disease: flow-cytometric measurement and clinical associations. Blood. 1996; 88:1873–1880.

31. Tait JF, Brown DS, Gibson DF, Blankenberg FG and Strauss HW.

Development and characterization of annexin V mutants with endogenous chelation sites for (99m)Tc. Bioconjug Chem. 2000; 11:918–925.

32. Mochizuki T, Kuge Y, Zhao S, Tsukamoto E, Hosokawa M, Strauss HW, Blankenberg FG, Tait JF and Tamaki N. Detection of apoptotic tumor response in vivo after a single dose of chemotherapy with ^{99m}Tc-annexin V. J Nucl Med. 2003; 44(1):92-7.

33. Brown RS, Leung JY, Fisher SJ, Frey KA, Ethier SP and Wahl RL. Intratumoral distribution of tritiated fluorodeoxyglucose in breast carcinoma. I. Are inflammatory cells important? J Nucl Med. 1995; 36:1854-1861.

34. Zhao S, Kuge Y, Mochizuki T, Takahashi T, Nakada K, Sato M, Takei T and Tamaki N. Biologic correlates of intratumoral heterogeneity in 18F-FDG distribution with regional expression of glucose transporters and hexokinase-II in experimental tumor. J Nucl Med. 2005; 46:794-799.

35. Johnson LL, Schofield L, Donahay T, Narula N and Narula J.

^{99m}Tc-annexin V imaging for in vivo detection of atherosclerotic lesions in porcine coronary arteries. J Nucl Med. 2005; 46: 1186 –1193.

36. Kietselaer BL, Reutelingsperger CP, Heidendal GA et al. Noninvasive detection of plaque instability with use of radiolabeled annexin A5 in patients with carotid-artery atherosclerosis. N Engl J Med. 2004; 350: 1472–1473.

37. Strauss HW, Mari C, Patt BE, Ghazarossian V. Intravascular radiation detectors for the detection of vulnerable atheroma. J Am Coll Cardiol. 2006 Apr 18; 47(8 Suppl):C97-100.

38. Isobe S, Tsimikas S, Zhou J, et al. Noninvasive imaging of atherosclerotic lesions in apolipoprotein E-deficient and low-density-lipoprotein receptor-deficient mice with annexin A5. J Nucl Med. 2006 Sep; 47(9):1497-505.

39. Grierson JR, Yagle KJ, Eary JF, Tait JF, Gibson DF, Lewellen B, Link JM, Krohn KA. Production of [F-18]fluoroannexin for imaging apoptosis with PET. Bioconjug Chem. 2004; 15: 373-379.

40. Smith-Jones PM, Afroze A, Zanzonico P, Tait J, Larson SM, Strauss

HW. 68GA labeling of Annexin-V: Comparison to 99mTc-Annexin-V and 67GA-Annexin. J Nucl Med. 44(5 supplement). May 2003. 49P-50P.

41. Zhuangyu Z, Josef M, Gerard H, et al. Non-invasive imaging of atherosclerotic plaque macrophage in a rabbit model with F-18 FDG PET: a histopathological correlation. BMC Nucl Med. 2006; 25.6-3.

42. Tawakol A, Migrino RQ, Bashian GG, et al. In vivo 18F-fluorodeoxyglucose positron emission tomography imaging provides a noninvasive measure of carotid plaque inflammation in patients. J Am Coll Cardiol. 2006 Nov 7; 48(9):1818-24. Epub 2006 Oct 17.

43. Rosenfeld ME, Polinsky P, Virmani R, Kauser K, Rubanyi G and Schwartz SM. Advanced atehrosclerotic lesions in the innominate artery of the ApoE knockout mouse. Arterioscler Thromb Vasc Biol. 2000; 20:2587-2592.

44. Schreyer SA, Vick C, Lystig TC, Mystkowski P, LeBoeuf RC. LDL receptor but not apoliporotein E deficiency increases diet-induced

obesity and diabetes in mice. *Am J Physiol Endocrinol Metab* 282: E207-E214, 2002.

45. Ohtsuki K, Hayase M, Akashi K, Kopiwoda S, Strauss HW. Detection of monocyte chemoattractant protein-1 receptor expression in experimental atherosclerotic lesions: an autoradiographic study. Circulation. 2001 Jul 10; 104 (2): 203 - 208.

46. Qin G, Zhang Y, Cao W, et al. Molecular imaging of atherosclerotic plaques with technetium-99m-labelled antisense oligonucleotides. Eur J Nucl Med Mol Imaging. 2005 Jan;32(1):6-14. Epub 2004 Nov 26.

47. Hartung D, Sarai M, Petrov A, et al. Resolution of apoptosis in atherosclerotic plaque by dietary modification and statin therapy. J Nucl Med. 2005 Dec ; 46 (12) : 2051-2056.

48. Johnson JL, Fritsche-Danielson R, Behrendt M, et al. Effect of broad-spectrum matrix metalloproteinase inhibition on atherosclerotic plaque stability. Cardiovasc Res. 2006 Aug 1; 71 (3):586-95. Epub 2006 May 10.

49. Mazzolai L, Duchosal MA, Korber M, et al. Endogenous angiotensin II

induces atherosclerotic plaque vulnerability and elicits a Th1 response in ApoE-/- mice. Hypertension. 2004 Sep;44 (3):277-82. Epub 2004 Aug 9

Figure legends

Figure 1 Example of ROI placement on autoradiographic image (**a**), Oil Red O staining (**b**-**e**), hematoxylin and eosin staining (**f**-**i**) and immunohistochemical staining for macrophage (**j**-**m**).

Histological grading of atherosclerotic lesion was performed based on the intensity of Oil Red O staining: 0 = not stained, 1 = slightly stained, 2 = intensely stained and 3 = very intensely stained. For testing feasibility of the histological grading based on Oil Red O staining, hematoxylin and eosin staining and immunohistochemical staining for macrophage were performed using aortic specimens corresponding to each grade of Oil red O staining. The variation of Oil Red O staining allowed us to stratify the lesions to those with high and low lipid content which partly indicated the levels of atherosclerosis progression, as confirmed by hematoxylin and eosin staining and immunohistochemical staining for macrophage. Bar = 100 μm.

Figure 2 Autoradiograms (ARG) and corresponding Oil Red O staining in aortas of ApoE-/- mice injected with ^{99m}Tc-annexin A5 (**a, b**) or ^{18}F-FDG (**c, d**).

The regions stained red with Oil Red O reveal the presence of atherosclerotic lesions. Corresponding autoradiography showed tracer accumulation in the atherosclerotic lesions matching with the Oil Red O staining.

Figure 3 Average uptake levels (%ID x kg/m^2) of ^{99m}Tc-annexin A5 and ^{18}F-FDG in aortic tissues of ApoE-/- and control mice.

Both tracers showed higher uptake levels in ApoE-/- mice than in control mice. ^{18}F-FDG showed higher absolute uptake levels than ^{99m}Tc-annexin A5 in both strains.

Figure 4 Correlation between regional tracer uptake level and lesion development in ApoE-/- mice.

The regional uptake levels of ^{99m}Tc-Annexin A5 (**a**) or ^{18}F-FDG (**b**) in the aortic tissues correlated with the atherosclerosis severity level determined by Oil Red O staining.

Figure 5 Relative tracer uptake level in aortic tissues of ApoE-/- mice. Relative uptake values (RUVs) were defined as the ratio of tracer uptake in each ROI group to that in the ROI group with Oil Red O staining scores of 0-0.5. The uptake ratios of advanced lesions (score, > 0.5) to early lesions (score, < 0.5) were significantly higher for ^{99m}Tc-annexin A5 than for ^{18}F-FDG ($f=4.73$, $p=0.03$).

TABLE 1

Body weight, and blood glucose and plasma lipid levels of apoE-/- and control mice given western type diet.

	ApoE-/- mice	Control mice	P-value
^{99m}Tc-annexin A5 group	n = 12	n = 11	-----
Body weight (gram)	47.1 ± 4.7	41.1 ± 3.6	<0.05
Blood glucose level (mg/dl)	125 ± 21	147 ± 27	<0.05
Plasma cholesterol level (mg/dl)	1767 ± 301	186 ± 21	<0.05
Triglycerides (mg/dl)	144 ± 16	40 ± 21	<0.05
^{18}F-FDG group	n = 14	n = 15	-----
Body weight (gram)	45.1 ± 5.9	39.9 ± 3.0	<0.05
Blood glucose level (mg/dl)	113 ± 18	139 ± 16	<0.05
Plasma cholesterol level (mg/dl)	1672 ± 450	175 ± 31	<0.05
Triglycerides (mg/dl)	120 ± 53	30 ± 16	<0.05
P-value	NS*	NS*	-----

Significantly higher body weight and plasma lipid levels were observed in ApoE-/- mice, whereas significantly higher blood glucose levels were observed in control mice. *No significant difference was observed in each parameter between ^{99m}Tc-annexin A5 and ^{18}F-FDG groups in the same strain.

TABLE 2

Atherosclerotic lesions developed in ApoE-/- and control mice.

	Oil Red O staining score	% of ROIs	
		^{99m}Tc-annexin A5	^{18}F-FDG
ApoE-/- mice	0 - 0.5	78.7±9.6	76.9±6.2
	0.5 - 1	5.4±2.4	8.6±4.7
	> 1	14.5±6.2	15.9±8.4
Control mice	0 - 0.5	100.0	100.0

No significant differences were observed in atherosclerotic lesion development between ^{99m}Tc-annexin A5 group and ^{18}F-FDG group ($f = 0.76$; $p = 0.48$).

Figure 1

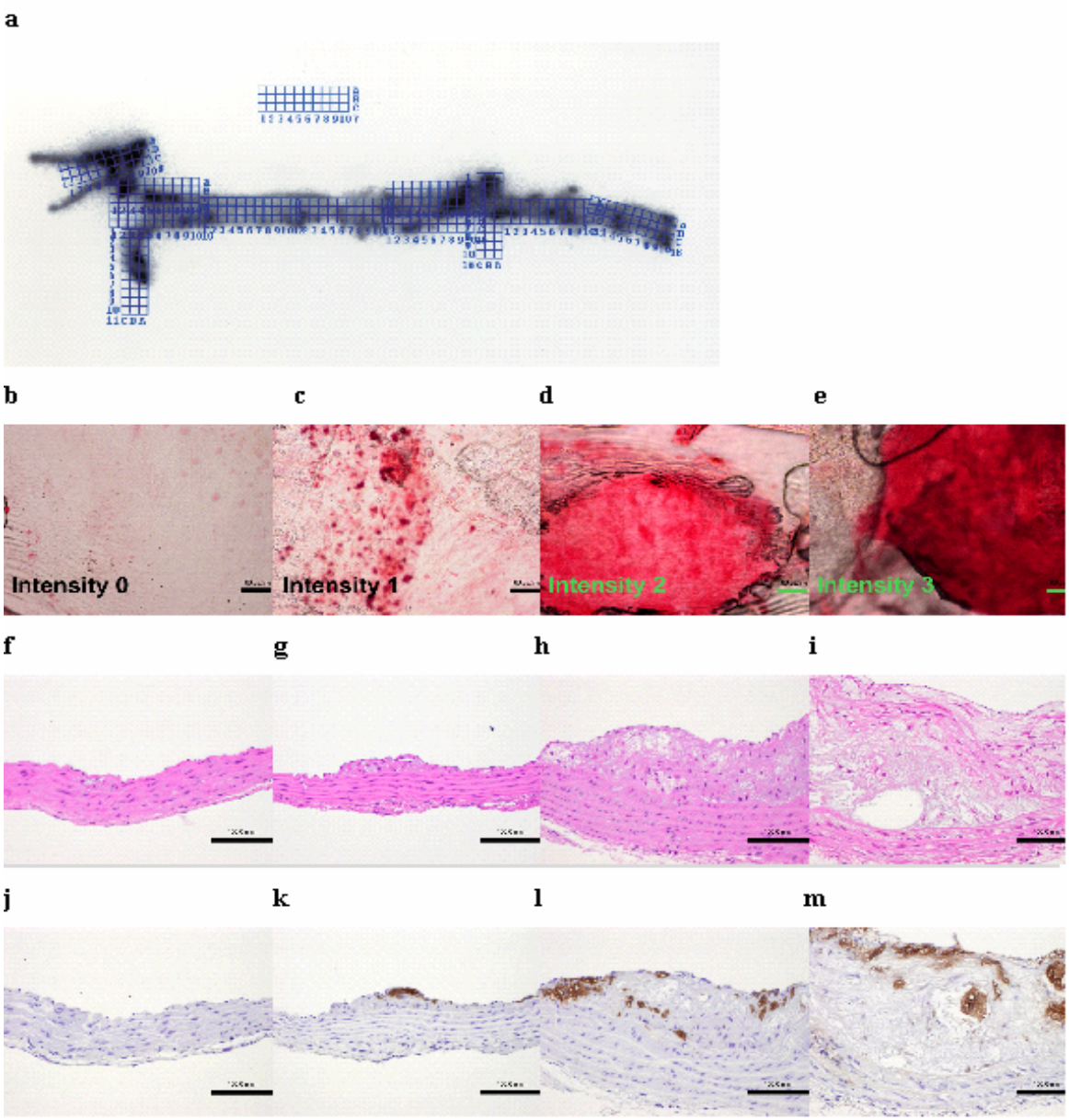
a
b
c
d
e
Intensity 0
Intensity 1
Intensity 2
Intensity 3
f
g
h
i
j
k
l
m

Figure 2.

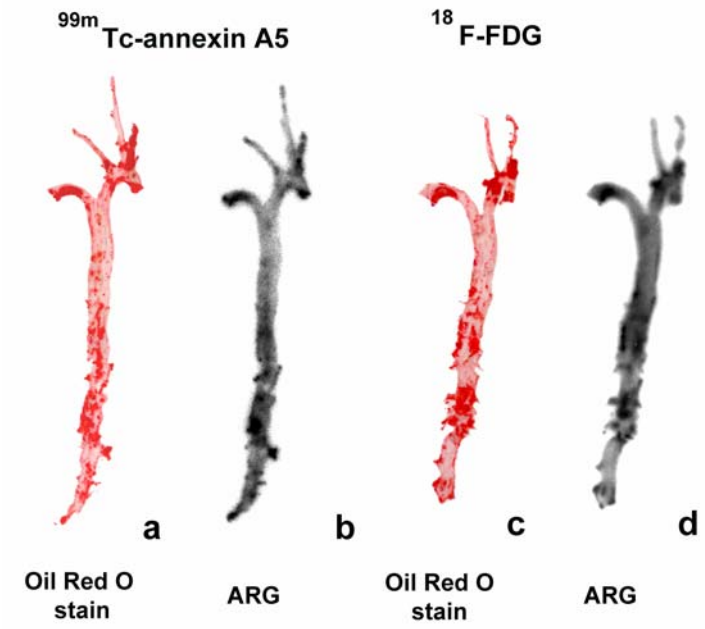
99m Tc-annexin A5
18 F-FDG
a
b
c
d
Oil Red O stain
ARG
Oil Red O stain
ARG

Figure 3

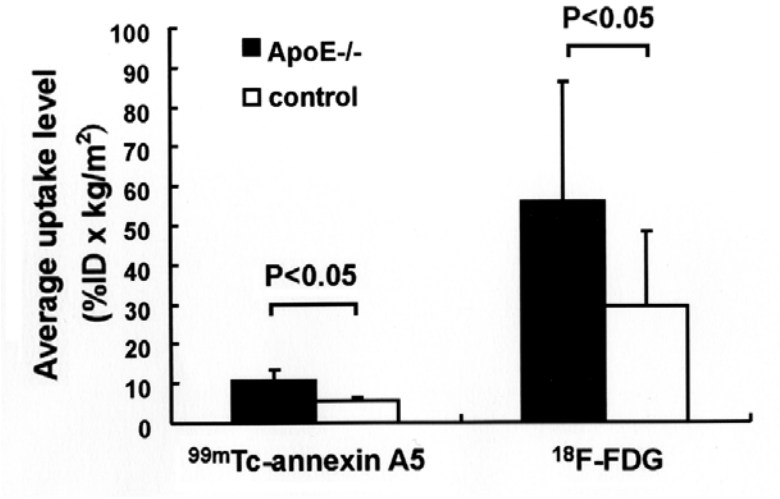
P<0.05
ApoE-/-
control
Average uptake level
(%ID x kg/m2)
100
90
80
70
60
50
40
30
20
10
0
P<0.05
99mTc-annexin A5
18F-FDG

Figure 4.

a.

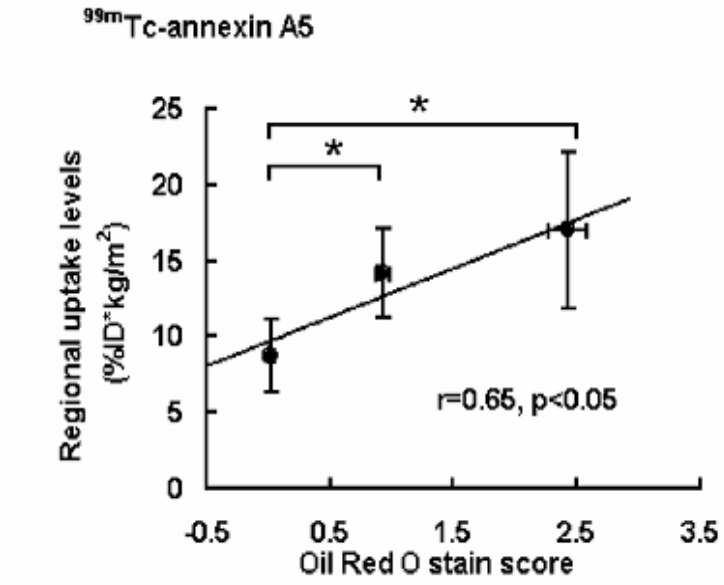
99mTc-annexin A5
Regional uptake levels (%ID*kg/m2)
25
20
15
10
5
0
*
*
r=0.65, p<0.05
-0.5
0.5
1.5
2.5
3.5
Oil Red O stain score

b.

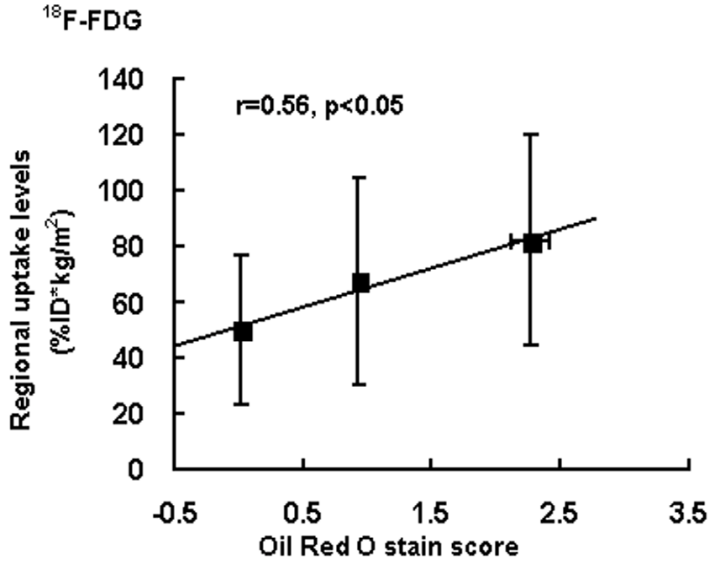
18F-FDG
Regional uptake levels (%ID*kg/m2)
140
120
100
80
60
40
20
0
r=0.56, p<0.05
-0.5
0.5
1.5
2.5
3.5
Oil Red O stain score

Figure 5

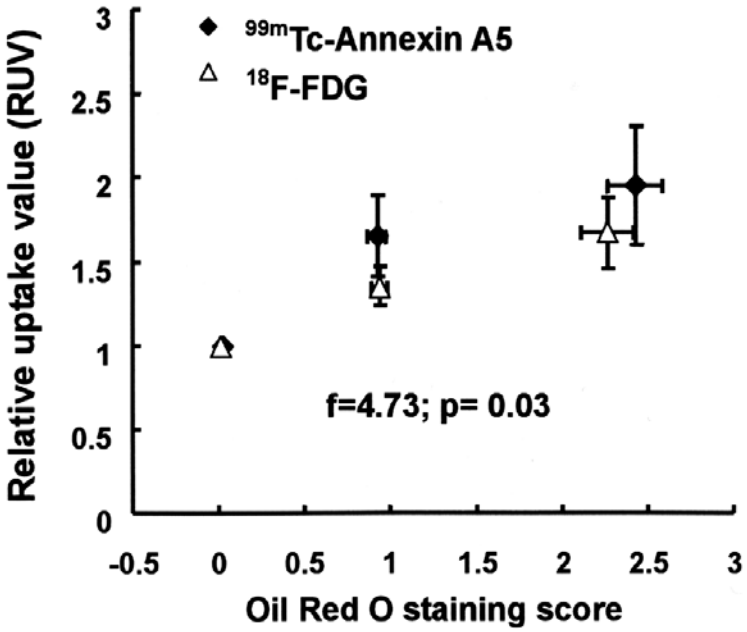
99mTc-Annexin A5
18F-FDG
f=4.73; p= 0.03
Relative uptake value (RUV)
Oil Red O staining score
3
2.5
2
1.5
1
0.5
0
-0.5
0
0.5
1
1.5
2
2.5
3